Available online at www.sciencedirect.com

SciVerse ScienceDirect

journal homepage: www.elsevier.com/locate/watres

Ambient iron-mediated aeration (IMA) for water reuse

Yang Deng [a,b], James D. Englehardt [a,*], Samer Abdul-Aziz [a,c], Tristan Bataille [a,d], Josenrique Cueto [a,e], Omar De Leon [a,f], Mary E. Wright [a], Piero Gardinali [a,g], Aarthi Narayanan [a,h], Jose Polar [a,i], Shibata Tomoyuki [a,j]

[a] Department of Civil, Architectural, and Environmental Engineering, University of Miami, Coral Gables, FL 33124, USA
[b] Department of Earth and Environmental Studies, Montclair State University, Montclair, NJ 07043, USA
[c] Zima Group International, PO BOX 565, Tripoli 1300, Lebanon
[d] Ecole Nationale des Travaux Publics de l'Etat, 69518 Vaulx-en-Velin cedex, France
[e] Hazen and Sawyer P.C., 999 Ponce De Leon Blvd., Suite 1150, Coral Gables, FL 33134, USA
[f] Environmental & Regulatory Advisor, ExxonMobil Development Company, 12450 Greenspoint Dr., Houston, TX 77060, USA
[g] Department of Chemistry and Biochemistry, Florida International University, Miami, FL 33199, USA
[h] Particle Engineering Research Center, University of Florida, Gainesville, FL 32611, USA
[i] ARCADIS U.S., Inc., 14025 Riveredge Drive, Suite 600, Tampa, FL 33637, USA
[j] Public Health Program and Institute for the Study of the Environment, Sustainability & Energy, Northern Illinois University, DeKalb, IL 60115, USA

ARTICLE INFO

Article history:
Received 22 August 2012
Received in revised form
31 October 2012
Accepted 5 November 2012
Available online 21 November 2012

Keywords:
Iron
Dissolved oxygen
Water reuse
Oxidation
Coagulation
Adsorption

ABSTRACT

Global water shortages caused by rapidly expanding population, escalating water consumption, and dwindling water reserves have rendered water reuse a strategically significant approach to meet current and future water demand. This study is the first to our knowledge to evaluate the technical feasibility of iron-mediated aeration (IMA), an innovative, potentially economical, holistic, oxidizing co-precipitation process operating at room temperature, atmospheric pressure, and neutral pH, for water reuse. In the IMA process, dissolved oxygen (O_2) was continuously activated by zero-valent iron (Fe^0) to produce reactive oxygen species (ROS) at ambient pH, temperature, and pressure. Concurrently, iron sludge was generated as a result of iron corrosion. Bench-scale tests were conducted to study the performance of IMA for treatment of secondary effluent, natural surface water, and simulated contaminated water. The following removal efficiencies were achieved: 82.2% glyoxylic acid, ~100% formaldehyde as an oxidation product of glyoxylic acid, 94% of Ca^{2+} and associated alkalinity, 44% of chemical oxygen demand (COD), 26% of electrical conductivity (EC), 98% of di-n-butyl phthalate (DBP), 80% of 17β-estradiol (E2), 45% of total nitrogen (TN), 96% of total phosphorus (TP), 99.8% of total Cr, >90% of total Ni, 99% of color, 3.2 log removal of total coliform, and 2.4 log removal of *E. Coli*. Removal was attributed principally to chemical oxidation, precipitation, co-precipitation, coagulation, adsorption, and air stripping concurrently occurring during the IMA treatment. Results suggest that IMA is a promising treatment technology for water reuse.

* *Corresponding author*. Tel.: +1 305 284 5557.
E-mail address: jenglehardt@miami.edu (J.D. Englehardt).
0043-1354
http://dx.doi.org/10.1016/j.watres.2012.11.005

1. Introduction

Rapidly expanding population, escalating water consumption, and dwindling water resources severely aggravate the water shortage problem at a global scale, particularly in arid and water-stressed areas, rendering water reuse a strategically significant approach to meet the current and future water demand (USEPA, 2004). Over the past decades, water reuse has been practiced to reclaim water for non-potable urban, industrial, and agricultural reuse, as well as augmentation of potable water supplies through indirect or direct reuse. A key question, during the selection of a water reclamation process, is whether wastewater can be adequately treated to ensure water quality appropriate for the intended uses. Although many treatment processes have been used in an effort to produce high quality reclaimed water, most of them, except membrane processes, cannot simultaneously remove a wide spectrum of contaminants in water in a single reactor. For example, advanced oxidation processes (AOPs) are generally ineffective for heavy metal removal because heavy metals cannot be decomposed like organic pollutants, though AOPs (e.g. photocatalytic oxidation) readily remove most of organic compounds in water via oxidation (Zhao et al., 2007). Another critical question is cost. A high capital or operating cost often significantly limits application of some technically effective treatment options in practice, such as energy-intensive membrane separation. Therefore, innovative and cost-effective technologies are highly needed for the further development of water reuse.

Our previous work (Benoit et al., 1997; Englehardt et al., 2001; Bataille, 2003; Mognol, 2004; Legrenzi, 2004; Englehardt et al., 2007) reported that zero-valent iron (Fe^0) treated an EDTA and heavy metal-containing water, and inactivated *E. coli*, under an air-aerated condition at ambient pH, temperature, and pressure. In the so-called iron-mediated aeration (IMA) process, dissolved oxygen was continuously activated by Fe^0 to produce reactive oxygen species (ROS) to degrade EDTA (>99%) and glyoxylic acid via oxidation, mechanistically different from Fe^0-based reductive remediation technologies. This finding is in agreement with other studies that demonstrated Fe^0 oxidation of the chlorinated aromatics 4-chlorophenol and pentachlorophenol in the presence of dissolved oxygen and EDTA (Noradoun et al., 2003). Other studies show slight oxidative addition of oxygen or alcohol groups to various organics in the absence of EDTA, at rates ranging from ~0.01 to 6% at treatment times from 1 to 24 h. Compounds tested include benzoic acid (Joo et al., 2005; Feitz et al., 2005; Keenan and Sedlak, 2008a, b), persistent pesticides (e.g. molinate, lindane, and atrazine) (Joo and Zhao, 2008; Feitz et al., 2005), and simple alcohols (e.g. methanol, ethanol, and 2-propanol). In terms of physical removal, on the other hand, we showed efficient simultaneous removal of toxic inorganic ions including chelated Hg^{2+}, Cd^{2+}, Pb^{2+}, and Ni^{2+}, and free arsenate, arsenite, Sr^{2+}, chromate, and vanadate due to co-precipitation by iron sludge (iron oxyhydroxides), the iron corrosion products (Englehardt et al., 2007). Of note, the ROS generation and physical treatment occur at atmospheric pressure, room temperature, and a broad pH range, without the aid of irradiation. Also, in contrast with conventional coagulation processes, the approach imparts no salts, e.g. sulfate or chloride, which might accumulate in low-energy closed-loop or partially closed-loop water reuse systems not employing reverse osmosis treatment. Furthermore, Fe^0 is a low-cost material, and atmospheric oxygen is readily available. Therefore, the IMA may be a promising option for water reuse.

The objective of this study was to evaluate the technical feasibility of IMA for removal of a broad suite of constituents in water reuse applications under ambient conditions. Bench-scale experiments were conducted to study the performance of IMA in the removal of chemical oxygen demand (COD), electrical conductivity (EC), endocrine disrupting compounds (EDCs), nutrients, calcium hardness, heavy metals, color, and microbial indicators from secondary wastewater effluent, natural water, or simulated contaminated water. As well, mechanisms behind the removal phenomena are proposed.

2. Materials and methods

All reagents were at least reagent grade and were used as received, and solutions were prepared with Milli-Q water (18.2 MΩ-cm), except as noted. Simulated natural water was prepared for hardness removal tests as 0.5 mM $CaCl_2$ and 1.63 mM $NaHCO_3$ in Milli-Q water, adjusted to pH 7.5 with concentrated HCl, and for the formaldehyde oxidation tests by aeration of 250 mg $CaCO_3$ in 1 L deionized water (DI) for 24 h. All bottles, glassware, and high-density polyethylene (HDPE) containers were acid washed (20% aqueous v/v, HNO_3, trace metal grade) prior to use. Specifically, all glassware for microbial tests was sterilized in an autoclave (Model: 120/208 240, Market Forge Co., Everett, Massachusetts) at 115 °C and 1200 kPa for 20 min before use.

All tests were conducted in an IMA test tube reactor, except for those for nitrogen and phosphorus removal. The IMA reactor configuration was shown in Fig. 1. Commercial steel wool (Brillo®) was prepared as the iron source by sequential hexane rinse, complete drying, 0.1 N HCl rinse, and final air drying. In a 30 mL test tube reactor, 1.0 g steel wool was

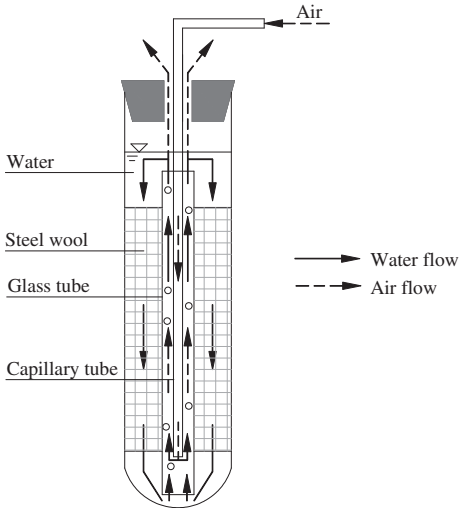

Fig. 1 – Schematic of the IMA test tube reactor.

arranged uniformly between the outer glass tube and the test tube wall. Solution was aerated with air that was pre-humidified by bubbling through Milli-Q water. The gas flow was controlled at 5 ± 1 mL/s during the entire treatment period. Gas was delivered through the inner tube to the annular space between the two glass tubes in the test tube center, creating vertical circulation of solution upward through the annular space and downward through the iron wool packing. Homogeneous circulation was verified using bromocresol purple dye. At each designated reaction time, at least, two reactors were sacrificed. The samples were vacuum filtered through 0.45 μm membrane filter prior to analysis.

In the nitrogen and phosphorus removal tests, 1 L secondary effluent was dispensed to 1 L beakers installed on a jar testing apparatus (Phipps & Bird, USA). Powdered iron, <10 μm, was added and the secondary effluent was aerated with an air pump at 3 L/min air flow and 1 L/min N_2 flow. The reactor was run in the following sequence: (a) 2 h flash mix with 100 g iron powder and aeration at 240 rpm, (b) 2 h covered rapid mix and nitrogen sparge at 200 rpm, and (c) 15 min flocculation at 10 rpm. After flocculation, a 60 mL aliquot was collected and vacuum filtered through 0.45 μm membrane filter. A second set was run likewise except for the addition of a 24 h quiescent, zero-headspace period prior to flocculation. In these tests, N_2 stripping and anoxic quiescence were provided as a test for possible reductive precipitation of vivianite from ferric hydroxyphosphate. In the tests for removal of COD, EC, and nutrients, secondary effluent was used, which was collected subsequent to secondary sedimentation and prior to chlorination from the Central District Wastewater Treatment Plant (Miami, Florida, USA). In the EDC oxidation tests, 1000 μg/L EDC solution was prepared by adding certain amount of 0.1 g di-n-butyl phthalate or 17-β-estrodiol/100 mL methanol to Milli-Q water. In the Ni and Cr removal tests, the metal-contaminated water was prepared by addition of certain amounts of $NiCl_2$ and K_2CrO_4 to simulated natural water. For color removal tests, Everglades-derived raw water typically containing humics and tannins was sampled from the Hialeah/Preston Water Treatment Plant (Hialeah, Florida, USA). In the total coliform inactivation tests, water was collected from Lake Osceola on the University of Miami campus (Coral Gable, Florida, USA). In *E. coli* inactivation tests, on the other hand, a water sample containing approximately 10^7 CFU/mL *E. coli* was prepared by dilution of a 10^9 CFU/mL *E. coli* solution with a phosphate buffer solution (dilution factor = 1:100). The 10^9 CFU/mL *E. coli* solution was prepared as follows. Pure strains of *E. coli* (Microbiologics, St Cloud, Minnesota) was inoculated on sterile plates with a nutrient agar media (8 g/L of nutrient broth and 20 g/L of agar (Bacto Agar 0140-01, Difco, Detroit, Michigan)) in an incubator (Model 4570101, Dayton Walther, Marvel Division, Dayton, Ohio) at 35 °C for 24 h. Subsequently, one spore colony was transferred to an Erlenmeyer flask with 50 mL of nutrient broth (DF0003-17, Difco Co., Detroit, Michigan). After 15-h incubation at 37 °C, the solution was vigorously mixed. The homogenous solution had an average concentration of ~10^9 CFU/mL *E. coli*.

Solution pH and EC were generally measured along with other water quality parameters. COD was analyzed colorimetrically (3–150 mg/L, HACH, Loveland, CO, USA). Cr and Ni were quantified using inductively coupled plasma-atomic emission spectroscopy (ICP/AES) following US EPA method 6010B at 284.325 and 221.647 nm, respectively. Total nitrogen (TN) concentrations of the untreated and treated samples were measured according to HACH method 10072 (10–150 mg/L) and 10071 (0.5–25 mg/L), respectively. Total phosphorous (TP) was measured spectrophotometrically in duplicate samples by Parkson Corporation, Ft. Lauderdale, FL, USA through an agreement with Florida Atlantic University. Color was quantified using the standard Visual Comparison Method. IDEXX's Colilert 18® reagents (IDEXX, Westbrook, MN) were used with a test well tray for enumeration of total coliform and *E. coli*. Glyoxylic acid was measured by the method of Caprio and Insola (1986). Formaldehyde was measured as a product of glyoxylic acid degradation, by the method of Josimovic (1972). Selected organic constituents (di-n-butyl-phthalate and 17-β-estradiol) were measured using micro liquid–liquid extraction of sample against methylene chloride. After concentration and derivatization with BSFTA, target analytes were detected by gas chromatography mass spectrometry (GC/MS) using a Thermo DSQ instrument operated in electronic impact mode (EI) (Thermo Fisher Scientific, San Jose, CA). At a minimum, all experiments were run in duplicate or triplicate. Error bars in the figures represent one standard deviation.

3. Results

3.1. Oxidation

In Fig. 2, the oxidation of glyoxylic acid in water by IMA, and by H_2O_2-enhanced IMA, is shown. The pH in these tests with glyoxylic acid was 4.4 initially, rising gradually to 4.9 at 9 h and 5.2 at 27 h. Though partitioning to the oxyhydroxide phase was not measured in this experiment, results are consistent with those presented for the oxidative pathway previously (Englehardt et al., 2007). In that work, oxidation was shown to be first order with respect to glyoxylic acid, and 0.0831-order with respect to the molar concentration of $Fe^{III}_{(s)}$ sludge. That is, oxidation was indicated to be slightly inhibited by the iron oxyhydroxide sludge phase as it accumulated in the reactor. Also, oxidation was not inhibited by the addition of 0.256 mM *p*-chlorobenzoic acid as a hydroxyl radical scavenger (pH 7.5, initial concentration 0.153 mM), effectively ruling out an OH-mediated mechanism in that case.

The removal of formaldehyde, the oxidative product of glyoxylic acid, is also shown in Fig. 2. Formaldehyde concentration peaked at 1.17 mM after IMA oxidation of 7 mM glyoxylic acid for 20 min, decreasing to 0.05 mM after 24 h, representing effectively complete removal of the formaldehyde produced. Because the solubility of formaldehyde in water is 400,000 mg/L, the removal of formaldehyde to below detection is presumably not by physical adsorption. Also, although volatile, formaldehyde is not stripped due to substantial hydration and a low Henry's Law constant. Moreover, because the timescale for removal by coagulation is on the order of minutes, whereas the formaldehyde disappears on a timescale of hours, removal is likely by oxidation. Hence, it is likely that other such easily oxidized organics as glyoxylic acid and formaldehyde may be subject to oxidation

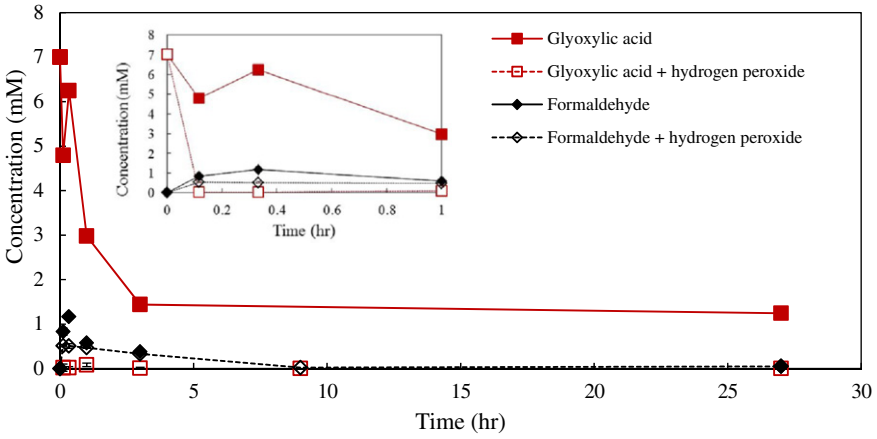

Fig. 2 – Oxidative removal of glyoxylic acid and its degradation product – formaldehyde product from water by IMA and H_2O_2-enhanced IMA. [Conditions: Initial concentration 7.0 mM glyoxylic acid in neutral saturated calcium carbonate buffer simulating natural water].

by IMA, whereas these oxidative pathways have not been noticed previously due to difficulties in distinguishing oxidation from physical removal, and to the longer timeframe required for oxidation.

3.2. *Softening, COD, electrical conductivity and EDCs*

In Fig. 3 the precipitation and removal of calcium hardness from simulated natural water by IMA is shown. Within 48 h, 94% of Ca^{2+} at an initial concentration of 27.15 mg/L was removed by the IMA. Precipitation of calcium carbonate also removed alkalinity, a hydroxyl radical scavenger that may interfere with downstream oxidative processes in water reuse applications. This removal was achieved along with reduction for other constituents as reflected by the decrease of EC with time, without the generation of salt brine requiring disposal. Of note, EC in the IMA group was slightly increased from 222 to 240 μs/cm from 9 to 48 h, probably because some water was lost as a result of the enhanced evaporation due to continuous bubbling, so that dissolved chemicals were concentrated. While these results are a function of the aqueous ionic balance, and hence specific to the water matrix, they are consistent with those of Chao and Westerhoff (2002) who termed the process *aeration softening*.

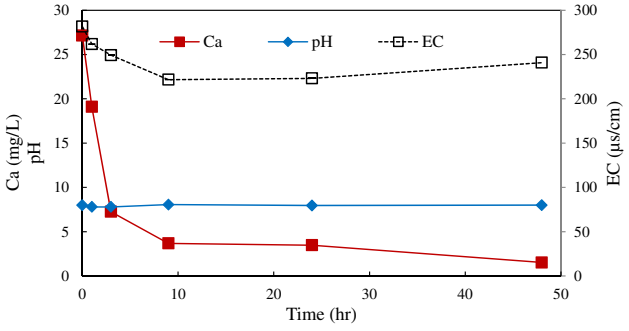

Fig. 3 – pH, Ca and conductivity in simulated natural water versus time in IMA [Conditions: Ca_0 = 27.2 mg/L; EC_0 = 281.6 μs/cm; and pH_0 = 7.99].

Reduction of residual COD and EC in secondary effluent with time in the IMA and control groups is shown in Fig. 4. The initial concentration of 50 mg/L COD was dramatically reduced to 56%, corresponding to 44% removal, within the first hour, and then slowly decreased to 34% in the following 26 h. In contrast, COD in the control group (no Fe^0 or air) gradually dropped and stabilized at 67% within 27 h, perhaps due to continued microbiological degradation. On the other hand, EC in the IMA-treated sample exhibited a similar two-phase removal pattern with COD. Within the first hour, EC was rapidly reduced to 90%. Thereafter, EC slightly declined to 74% (26% removal) at 27 h.

Results in terms of the removal of two individual EDCs, DBP and E2, in IMA and control (air aeration alone) groups, are shown in Fig. 5. Although IMA and air aeration alone both achieved 98% removal of DBP within 24 h, different removal patterns were observed in the initial reaction stage. After 2 h, residual DBP concentrations were 15% and 68% of the initial 1000 μg/L, in the IMA and control groups respectively. This difference suggests that air stripping was not the only mechanism responsible for DBP removal. Similarly, at any particular reaction time, IMA treatment showed a higher E2 removal

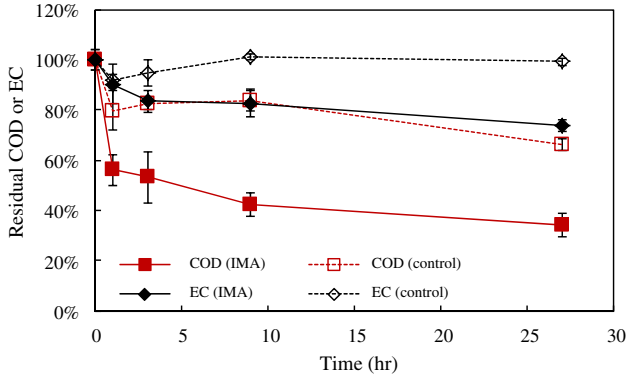

Fig. 4 – Residual COD and EC in secondary effluent versus time in IMA and control group (no Fe^0 or air aeration) [Conditions: COD_0 = 50 mg/L; EC_0 = 2.14 ms/cm; and pH_0 = 6.92].

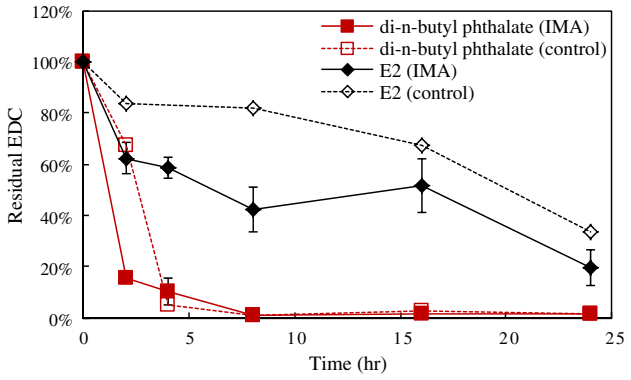

Fig. 5 – Residual di-n-butyl phthalate and 17β-estradiol versus time in IMA and control (air aeration alone) groups. [Conditions: C_0 = 1000 μg/L; pH ~ 7.5; control, air stripping alone without and reaction time = 25 h].

than air aeration alone (control). For example, residual E2 concentrations in the IMA and control groups were 20% and 33% of the initial 1000 μg/L, respectively, implying that part of E2 was removed by other mechanisms. In this IMA system, oxidation due to formation of active oxidizing agents and/or adsorption due to production of iron oxyhydroxide sludge were considered most likely to play a critical role in the additional removal of these EDCs.

3.3. *Total nitrogen and phosphorus*

Results of the IMA removal of TN and TP are shown in Fig. 6. Within 2 h TN decreased considerably from 33.8 to 18.5 mg/L, corresponding to a removal efficiency of 45%. No further removal was seen with the addition of an anoxic quiescent period (to promote vivianite precipitation), as expected. TP was reduced from 0.48 mg/L to 0.32 mg/L in 2 h, and to 0.26 mg/L after an additional 24-h quiescent period. Moreover, 0.57 mg/L TP was reduced using simple IMA to an average of 0.021 mg/L, representing 96% removal in 24 h. The consistency of TP removal across two different reactor designs and iron sources, independent of anoxic treatment, suggests that the reactions are promoted specifically through IMA-induced mechanisms. Removal of nitrogen is important to meet potable water quality standards, and removal of both may be important in terms of preventing salt accumulation in low-energy potable reuse systems without environmental buffer.

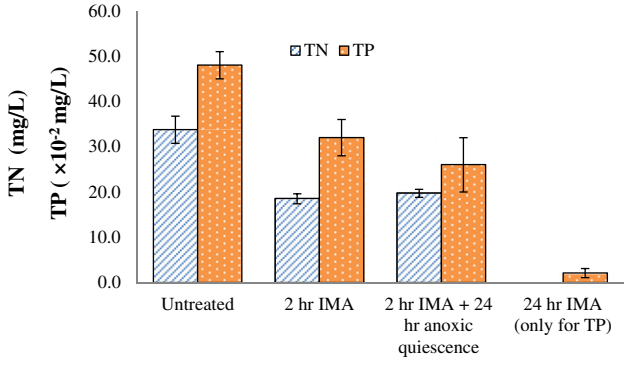

Fig. 6 – Residual total N and total phorspous in untreated and IMA treated secondary effluent at different times. [Conditions: Initial concentrations TP_0 = 0.48 mg/L and 0.57 mg/L, for 2-hour IMA (with and without anoxic quiescent period) and 24-hour IMA, respectively.]

3.4. *Heavy metals*

Fig. 7 shows the concurrent removal of total Cr and total Ni by IMA. Aeration only (control) did not remove Cr and Ni, indicating that O_2 oxidation and air sparging were ineffective for removal of the metals. However, IMA achieved a high reduction in Cr and Ni. The Cr concentration almost linearly declined with time, and the residual Cr was only 0.2% of the initial level (99.8% removal) after 27 h. Meanwhile, the residual Ni was below 10% of the initial level at 27 h, corresponding to >90% removal.

3.5. *Color*

Removal of secondary effluent color through IMA, Fe^0 only, aeration only, and control (no Fe^0 or aeration) are shown in Fig. 8. Neither aeration only nor control (no Fe/no aeration) treatments could remove significant color from the secondary effluent within 27 h, indicating that the color-causing compounds could not be degraded by O_2. When Fe only was used, color was rapidly increased to 195% of the initial level (100 unit) at 3 h, perhaps due to the release of iron ions as a result of Fe^0 oxidation by dissolved oxygen. Thereafter, the color gradually dropped and reached 50% at 27 h, possibly because the iron ions were subsequently precipitated as iron oxyhydroxides, partially sorbing color-causing compounds. In contrast, the color reduction by IMA was pronounced, exhibiting a nearly pseudo first-order reaction pattern with a rate constant of 0.09 h^{-1}(R^2 = 0.86). After 27 h, residual color fell to 1% of the initial level.

3.6. *Bacterial indicators*

Results in terms of log removal of total coliform from a lake water, and of *E. coli* from a phosphate buffer solution, are

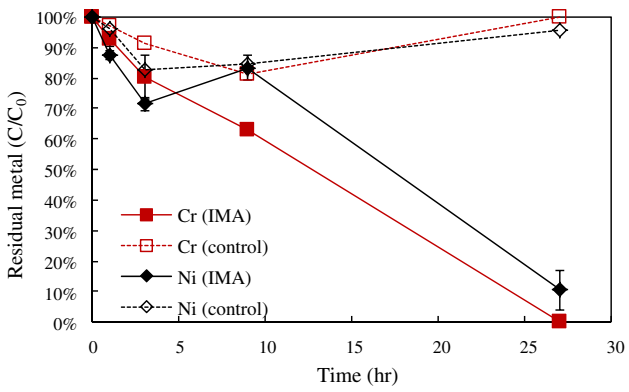

Fig. 7 – Simultaneous removal of total dissolved Cr and Ni in simulated natural water versus time in IMA and control (aeration only) [Conditions: initial Cr = 4.71 mg/L; initial Ni = 0.89 mg/L; and pH ~7].

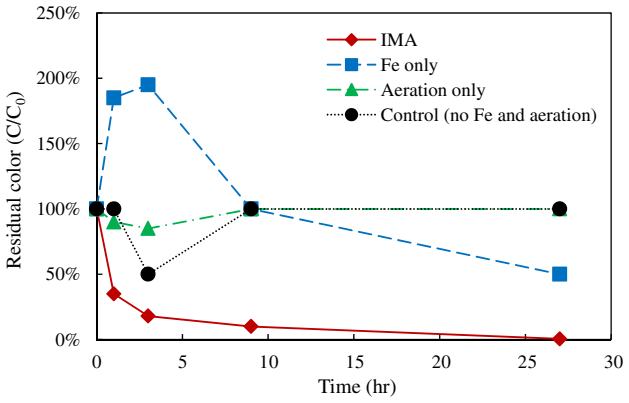

Fig. 8 – Color removal from the Everglades water versus time in IMA, Fe^0 only, aeration only, and control (no Fe^0 and no aeration) [Conditions: initial color = 100 unit; and pH = 7.7–8.6].

shown in Fig. 9. Removal of total coliform in the lake water increased with time, with log inactivation increasing from 1.7 at 5 min, to 3.2 after 60 min. Similarly, log inactivation of *E. coli* also increased with time, reaching 2.4 after 140 min, much greater than the <0.2 log removal observed for the control group (no Fe^0 or aeration).

4. Discussion

The reduction in concentrations of chemical constituents and microbiological indicators mentioned above, taken together with previous results showing the oxidation of EDTA and associated organics and removal of cationic and anionic inorganics (Englehardt et al., 2007) might be ascribed to two complimentary mechanisms simultaneously occurring in the IMA system: 1) oxidation induced by ROS; and 2) coagulation, adsorption, and precipitation due to formation of iron sludge.

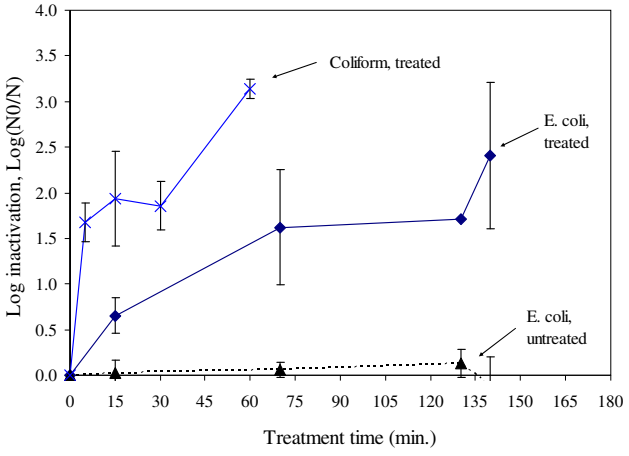

Fig. 9 – Removal of total coliforms in lake water and *E. coli* in a phosphate buffer solution [Condition: initial total coliform in the lake water = 13,755 MPN/100 mL; initial *E. coli* = 10^7 CFU/mL; and pH ~7; no Fe^0 and no aeration in the control].

4.1. *ROS-driven oxidation*

ROS-induced oxidation, rather than air sparging or adsorption by Fe^0 and its corrosion products, was verified to be responsible for removal of certain aqueous organic pollutants in previous works (Noradoun et al., 2003; Englehardt et al., 2007). Although the nature of ROS in the IMA is still unclear, the ROS production most likely involves the three sequential steps: Fe^0 oxidation, formation of H_2O_2 and Fe(II), and ROS production through Fenton-like chemistry. Initially, under the attack of O_2 or with the reaction of H^+ at acidic condition, Fe^0 is oxidized to release Fe(II) into the bulk solution. Unlike the traditional Fenton system based on direct addition of Fe(II) and H_2O_2, Fe^0 in the IMA, serving as a continuous Fe(II) source, gradually produces Fe(II) that participates in ROS production. Additionally, it is likely that some Fe(II) is produced through Fe(III) reduction by Fe^0 during the reaction. Then, H_2O_2 formation may occur via three plausible pathways. In the first mechanism, O_2 is reduced by Fe^0 to produce H_2O_2 involving formation of peroxide anion (O_2^{2-}) and hydroperoxide anion (HO_2^-), through consecutive two-electron transfer reactions as follows (Keenan and Sedlak, 2008a, b).

$$Fe(0) + O_2 \rightarrow Fe(II) + O_2^{2-} \quad (1)$$

$$O_2^{2-} + H^+ \rightarrow HO_2^- \quad (2)$$

$$HO_2^- + H^+ \rightarrow H_2O_2 \quad (3)$$

In the second pathway, Fe(II) reduces O_2 through a series of 1-electron reactions involving in the formation of superoxide ($O_2^{\bullet-}$) (Eq. (4) and (5)) (Biaglow and Kachur, 1997; Englehardt et al., 2007; Keenan and Sedlak, 2008a, b). However, Reaction (4) is a rate-limiting step, in which the 1-electron transfer to O_2 is not a thermodynamically favorable path for O_2 reduction ($E_0 = -0.33$ V for $O_2/O_2^{\bullet-}$) (Naqui et al., 1986).

$$Fe(II) + O_2 \rightarrow Fe(III) + O_2^{\bullet-} \quad (4)$$

$$Fe(II) + O_2^{\bullet-} + 2H^+ \rightarrow Fe(III) + H_2O_2 + 2OH^- \quad (5)$$

The third pathway is a direct two-electron reduction of O_2 by Fe(II) to generate H_2O_2 (Eq. (6)) (Biaglow and Kachur, 1997).

$$2Fe(II) + O_2 + 2H^+ \rightarrow 2Fe(III) + H_2O_2 \quad (6)$$

This process is more favorable thermodynamically ($E_0 = +0.30$ V for $O_2/O_2^{\bullet-}$) than Eq. (4).

Theoretically, ROS is finally produced from the reactions between Fe(II) and H_2O_2, the so-called Fenton reagents. Two parallel mechanisms initially proposed in the 1930s (Bray and Gorin, 1932; Haber and Weiss, 1934), the classical free radical and non-classical non-radical pathways, have been proposed to explain the Fenton chemistry, in which either hydroxyl radicals (OH•) or ferryl ion (Fe(IV)) are proposed as the principal ROS, respectively. Since then, the nature of ROS in the Fenton system has been a controversial issue for several decades. For the Fe^0/O_2 system, several efforts using radical scavenging tests were made to determine whether OH• or Fe(IV) is generated, but results varied with the different probe compounds used (Joo et al., 2005; Englehardt et al., 2007; Keenan and Sedlak, 2008a, b; Pang et al., 2011). However, hydroxyl radical

and ferryl ion are both strong oxidizing species, reactive towards numerous aqueous species. For example, the measured $OH^{\bullet}$ rate constants with effluent organic matters (EfOM) range from 0.27×10^9 to 1.21×10^9 M_C^{-1} s^{-1}, with an average value of $0.86 \pm 0.35 \times 10^9$ M_C^{-1} s^{-1} (Rosario-Ortiz et al., 2008). As a result, it is possible that IMA may have partially oxidized some organics in addition to formaldehyde, in this study, perhaps including EfOM, EDCs, and color-causing species. That is, the ROS produced through Fenton chemistry may play an important role. For example, Nakrst et al. (2011) reported that the Fenton process was very effective for the oxidation of EDCs (e.g. E2). Moreover, the oxidation is useful for oxidative removal of some toxic inorganics, such as As(III). Hug and Leupin (2003) reported that Fe^0 in an aerated water could oxidize As(III) to less toxic and mobile As (V), and the latter was easily adsorbed to the surface of iron oxyhydroxides. As well, based on comparison with results for conventional coagulation, inactivation of total coliform and *E. coli* was apparently at least partially associated with oxidation. For example, overall *E. coli* log removal achieved by the sequence of coagulation, flocculation and sedimentation is reported to be as high as 1.7 (Harrington, 2001), much less than 3.2 observed in this study, suggesting the role of oxidation in the removal of bacteria indicators. Also, Kim et al. (2010) recently conducted a successful study in direct inactivation of MS2 coliphage by Fenton oxidation, and found that the process was controlled by pH and iron-chelating agents.

4.2. *Iron sludge-driven precipitation, coagulation and adsorption*

Accompanying the Fe^0 corrosion during IMA, iron sludge is built up on the Fe^0 surface. These iron oxides likely play a vital role in improvement of the water quality. Overall, there are 16 known iron oxides/hydroxides, and the formation of every type is sensitively influenced by reaction conditions and water chemistry (Cornell and Schwertmann, 2003). Although chemical composition of the iron sludge was not identified in this study, the sludge produced was likely a mixture of different iron oxides/oxyhydroxides. Sarin et al. (2004) reviewed the growth, formation and structure of most iron corrosion products under oxic condition. Formation of iron corrosion layers starts with dissolved O_2 oxidation of Fe^0, as mentioned in 4.1. It is noted that as the corrosion proceeds, dissolved O_2 continuously diffuses from the bulk water towards the Fe^0 surface, while a flux of Fe(II), the product of Fe^0 oxidation, moves from the Fe^0 surface into the bulk water. With increasing thickness of the layer of iron corrosion products, diffusion of dissolved O_2 to the Fe^0 surface becomes increasingly difficult. In localized anoxic sites (e.g. next to the Fe^0 surface), H^+ may take over the oxidation, and accept electrons from Fe^0 to form $H_{2(g)}$. Another pathway to drive Fe^0 oxidation involves the conduction of electrons produced in Fe^0 oxidation through the iron sludge layer to a point where they may contact dissolved O_2. Fe(II) adsorbed to the iron sludge solids may also facilitate the electron conduction (Stratmann and Muller, 1994). On the other hand, Fe (II), once formed from the Fe^0 oxidation, can be transported outward from the Fe^0 surface to the bulk solution through the pore water in the iron corrosion products. Even in a O_2-rich water, the ferrous ions may successfully diffuse into the bulk water, and then be oxidized into Fe(III) oxide particles. This is confirmed by formation of small brown ferric iron flocs seen in the bulk water in this study. Of note, the average oxidation state of iron typically increases with distance from the Fe^0 surface, because the Fe(II) ions cannot be immediately oxidized when they transport into the bulk water. As a result, different iron corrosion products are formed in different iron sludge layers. Huang and Zhang (2005) found that the coating on the Fe^0 in the presence of dissolved oxygen was a dual thin layer with an inner maghemite (Fe_3O_4) layer (above the Fe^0 surface) preferably produced under anoxic condition, and an outer lepidocrocite(γ-FeOOH) layer (near the bulk solution) favorably formed under oxic condition.

In this study, the iron sludge layer is postulated to have had characteristic structure similar to that of pipe scales, a mixed iron corrosion product. This structure is typically composed of porous cores above the Fe^0 surface, a dense shell-like layer and a loose top surface layer. The cores are a porous mass with numerous small particles. Sarin et al. (2001) found that a high level of Fe(II) was present in the layer, with the forms of dissolved ferrous ions in pore water or solids such as $Fe(OH)_2$. A shell-like layer in such a scale is dominated by Fe_3O_4 and α-FeOOH (Sarin et al., 2001). However, such layers were likely absent or very thin in this study, because the shells are typically thinned at a fast iron corrosion and growth rate (Sarin et al., 2004). The top layer is mostly composed of loosely held particles of iron oxides such as amorphous $Fe(OH)_3$, along with some precipitates of phosphates and carbonates (Herro and Port, 1993; Sarin et al., 2001). Loose iron particles may also slough off the layer and enter bulk solution, thus contributing to iron floc-like particles.

During, and subsequent to, the formation of various iron oxides as iron sludge in the IMA system, different contaminants in secondary effluent may be removed through different mechanisms. Precipitation and co-precipitation likely dominate for reduction of electrical conductivity, as well as total dissolved solids (TDS), through conversion of soluble species into solids that can be readily removed by sedimentation. Particularly, ferric ions produced in the Fe^0 oxidation are well known to precipitate phosphorus into insoluble ferric phosphate (Davis and Cornwell, 2006). Coagulation, flocculation and adsorption also enhance the quality of the treated secondary effluent. In practice, their respective contributions to removal of a particular contaminant are difficult to determine. Coagulation and flocculation are especially effective for removal of insoluble (settable and colloidal) EfOM that on average accounts for 14% of total COD in secondary effluent (Shon et al., 2006). These mechanisms, along with co-precipitation, may also partially remove soluble EfOM. Abdessemed and Nezzal (2002) and Shon et al. (2004) achieved 77% and 57% removal of COD from EfOM using iron salt-induced coagulation/flocculation, respectively. Tchobanoglous and Burton (1991) also reported that such an iron salt-induced coagulation/flocculation could remove 30–60% of COD from EfOM. Accompanying coagulation and flocculation, adsorption may transfer organic or inorganic matters, particularly some emerging pollutants, from water to the iron sludge produced. For example, Figueroa and Mackay (2005) found that sorption of oxytetracycline (OTC) on hematite and goethite occurred principally via an inner sphere mechanism. Iron oxides might also play a vital role in

removal of inorganic pollutants. Tyrovola et al. (2006) reported that Fe^0 corrosion reactions caused high As(III) and As(V) uptake as a result of formation of inner-sphere, bidentate As(III) and As(V) complexes on the surfaces of Fe^0 and its corrosion products with the predominant As–Fe interatomic distances of 3.30–3.36Å.

5. Conclusions

Iron-mediated aeration is shown in this study to simultaneously remove a variety of organic and inorganic chemical constituents (cationic, anionic, and neutral) and bacterial indicators via chemical oxidation, precipitation, co-precipitation, coagulation, volatilization, and adsorption. This distinctive capacity is ascribed largely to the production of ROS and the formation of iron oxyhydroxide sludge during the IMA process. In contrast with conventional coagulation processes, the process imparts no salts to the water, making it particularly interesting in closed or partially closed-loop potable reuse applications in which salts may accumulate. In general, results are promising for the application of IMA to water and wastewater treatment. In particular, IMA when coupled with low-energy membrane filtration may offer holistic removal of organics, inorganics, and some salts, without the addition of sulfates or chlorides, in potable and non-potable water reuse applications. Further study of reactor design is recommended, including the use of low-cost iron sources.

Acknowledgments

Joel Mognol, Yves Legrenzi, Tommy Kiger, Erik Gadzinski, Patrick Kelly, Andrew Silverman, Felipe Behrens, Amir Zahir, and Bader Alessa are greatly appreciated for their IMA experiments at University of Miami. Special thanks to Mr. Doug Wachter (Vice President, Parkson Corporation, Ft. Lauderdale, FL) for analysis of total phosphorus. The National Science Foundation and the U.S. Environmental Protection Agency, NSF Award ID 1038257, and the University of Miami are gratefully acknowledged for partial support of this work.

REFERENCES

Abdessemed, D., Nezzal, G., 2002. Treatment of primary effluent by coagulation adsorption–ultrafiltration for reuse. Desalination 152 (1–3), 367–373.

Bataille, T., 2003. Investigation of Iron-mediated Aeration for Disinfection. Technical Report. Department of Civil, Architectural, and Environmental Engineering, University of Miami, Miami, FL, USA.

Benoit, B., Catilu, V., Herrera, A., Javorka, C., Kormienko, M., Lutchmansingh, T., MacNeal, D., Meeroff, D., Qi, X., Stebbins, J., Wark, R., Wilcox, W., 1997. Bench Study of The Effect of Zero-valent Iron on EDTA and Cadmium for In-situ Cleanup of Metals in Groundwater and Soil. Technical Report. Department of Civil, Architectural, and Environmental Engineering, University of Miami, Miami, FL, USA.

Biaglow, J.E., Kachur, A.V., 1997. The generation of hydroxyl radicals in the reaction of molecular oxygen with polyphosphate complexes of ferrous ion. Radiation Research 148 (2), 181–187.

Bray, W.C., Gorin, M.H., 1932. Ferryl ion, a compound of tetravalent iron. Journal of the American Chemical Society 54 (5), 2124–2125.

Caprio, V., Insola, A., 1986. A revised method for the spectrophotometric determination of glyoxylic acid. Analytica Chimica Acta 189, 379–382.

Chao, P.F., Westerhoff, P., 2002. Assessment and optimization of chemical and physicochemical softening processes. Journal of the American Water Works Association 94 (3), 109–119.

Cornell, R.M., Schwertmann, U., 2003. The Iron Oxides: Structure, Properties, Reactions, Occurrences and Uses, second ed. Wiley-VCH.

Davis, M., Cornwell, D., 2006. Introduction to Environmental Engineering, fourth ed. McGraw-Hill Science/Engineering/Math.

Englehardt, J., Echegoyen, L.D., Meeroff, D., 2001. In-situ chelation and removal of subsurface metals. In: Presented at Industry Partnerships for Environmental Science and Technology Conference, U.S. Department of Energy, National Energy Technology Laboratory, Morgantown, WV, USA.

Englehardt, J.D., Meeroff, D., Echegoyen, L., Deng, Y., Raymo, F., Shibata, T., 2007. Oxidation of aqueous EDTA and associated organics and coprecipitation of inorganics by ambient iron-mediated aeration. Environmental Science and Technology 41 (1), 270–276.

Feitz, A.J., Joo, S.H., Guan, J., Sun, Q., Sedlak, D.L., Waite, T.D., 2005. Oxidative transformation of contaminants using colloidal zero-valent iron. Colloid Surface A 265 (1–3), 88–94.

Figueroa, R.A., MacKay, A.A., 2005. Sorption of oxytetracycline to iron oxides and iron oxide-rich soils. Environmental Science and Technology 39 (17), 6664–6671.

Haber, F., Weiss, J., 1934. The catalytic decomposition of hydrogen peroxide by iron salts. Proceedings of the Royal Society of London: A Mathematical 147 (861), 332–351.

Harington, G.W., 2001. Removal of Emerging Waterborne Pathogens. AWWA Research Foundation.

Herro, H.M., Port, R.D., 1993. The Nalco Guide To Cooling Water System Failure Analysis. McGraw-Hill, New York.

Huang, Y.H., Zhang, T.C., 2005. Effects of dissolved oxygen on formation of corrosion products and concomitant oxygen and nitrate reduction in zero-valent iron systems with or without aqueous Fe^{2+}. Water Research 39 (9), 1751–1760.

Hug, S.J., Leupin, O., 2003. Iron-catalyzed oxidation of arsenic(III) by oxygen and by hydrogen peroxide: pH-dependent formation of oxidants in the Fenton reaction. Environmental Science and Technology 37 (12), 2734–2742.

Joo, S.H., Zhao, D., 2008. Destruction of lindane and atrazine using stabilized iron nanoparticles under aerobic and anaerobic conditions: effects of catalyst and stabilizer. Chemosphere 70 (3), 418–425.

Joo, S.H., Feitz, A.J., Sedlak, D.L., Waite, T.D., 2005. Quantification of the oxidizing capacity of nanoparticulate zero-valent iron. Environmental Science and Technology 39 (5), 1263–1268.

Josimovic, L., 1972. Determination of traces of formaldehyde, glyoxylic and glycolic acids in acetic acid-water mixtures. Analytica Chimica Acta 62, 210–213.

Keenan, C.R., Sedlak, D.L., 2008a. Factors affecting the yield of oxidants from the reaction of nanoparticulate zero-valent iron and oxygen. Environmental Science and Technology 42 (4), 1262–1267.

Keenan, C.R., Sedlak, D.L., 2008b. Ligand-enhanced reactive oxidant generation by nanoparticulate zero-valent iron and oxygen. Environmental Science and Technology 42 (18), 6936–6941.

Kim, J.Y., Lee, C., Sedlak, D.L., Yoon, J., Nelson, K.L., 2010. Inactivation of MS2 coliphage by Fenton's reagent. Water Research 44 (8), 2647–2653.

Legrenzi, Y., 2004. Investigation of Fibrous Media Mineral-mediated Aeration Reactor for Landfill Leachate Treatment. Technical report. Department of Civil, Architectural, and Environmental Engineering, University of Miami, Miami, FL, USA.

Mognol, J., 2004. Investigation of Fluidized Bed Mineral-mediated Aeration Reactor for Landfill Leachate Treatment. Technical Report. Department of Civil, Architectural, and Environmental Engineering, University of Miami, Miami, FL, USA.

Nakrst, J., Bistan, M., Tisler, T., Zagorc-Koncan, J., Derco, J., Gotvajn, A.Z., 2011. Comparison of Fenton's oxidation and ozonation for removal of estrogens. Water Science and Technology 63 (10), 2131–2137.

Naqui, A., Chance, B., Cadenas, E., 1986. Reactive oxygen intermediates in biochemistry. Annual Review of Biochemistry 55, 137–166.

Noradoun, C., Engelmann, M.D., McLaughlin, M., Hutcheson, R., Breen, K., Paszczynski, A., Cheng, I.F., 2003. Destruction of chlorinated phenols by dioxygen activation under aqueous room temperature and pressure conditions. Industrial and Engineering Chemistry Research 42 (21), 5024–5030.

Pang, S., Jiang, J., Ma, j, 2011. Oxidation of sulfoxides and arsenic(III) in corrosion of nanoscale zero valent iron by oxygen: evidence against ferryl ions (Fe(IV)) as active intermediates in Fenton reaction. Environmental Science and Technology 45, 307–312.

Rosario-Ortiz, F., Mezyk, S., Doud, D.R., Snyder, S.A., 2008. Correlation of absolute hydroxyl radical rate constants with non-isolated effluent organic matter bulk properties in water. Environmental Science and Technology 42, 5924–5930.

Sarin, P., Snoeyink, V.L., Bebee, J., Kriven, W.M., Clement, J.A., 2001. Physico–chemical characteristics of corrosion scales in old iron pipes. Water Research 35, 2961–2969.

Sarin, P., Snoeyink, V.L., Lytle, D.A., Kriven, W.M., 2004. Iron corrosion scales: model for scale growth, iron release, and colored water formation. Journal of Environmental Engineering, 364–373.

Shon, H.K., Vigneswaran, S., Kim, I.S., Cho, J., Ngo, H.H., 2004. The effect of pretreatment to ultrafiltration of biologically treated sewage effluent: a detailed effluent organic matter (EfOM) characterization. Water Research 38 (7), 1933–1939.

Shon, H.K., Vigneswaran, S., Snyder, S.A., 2006. Effluent organic matter (EfOM) in wastewater: constituents, effects, and treatment. Critical Reviews in Environmental Science and Technology 36, 327–374.

Stratmann, M., Muller, J., 1994. The mechanism of the oxygen reduction on rust-covered metal substrates. Corrosion Science 36 (2), 327–359.

Tchobanoglous, G., Burton, F.L., 1991. Wastewater Engineering: Treatment, Disposal, and Reuse, third ed. McGraw-Hill, New York.

Tyrovola, K., Nikolaidis, N.P., Veranis, N., Kallithrakas-Kontos, N., Koulouridakis, P.E., 2006. Arsenic removal from geothermal waters with zero-valent iron – effect of temperature, phosphate and nitrate. Water Research 40 (12), 2375–2386.

USEPA, 2004. Guidelines for Water Reuse. EPA/625/R-04/108.

Zhao, H., Jiang, D., Zhang, S., Wen, W., 2007. Photoelectrocatalytic oxidation of organic compounds at nanoporous TiO_2 electrodes in a thin-layer photoelectrochemical cell. Journal of Catalysis 250(), 102–109.